CFD Analysis of Double Pipe Heat Exchanger: A Comparative Study of Parallel and Counter Flow Configurations

Dhaygude Shubham Chandrakant[1], Hegadkar Shubham[2], Holkar Atharva Vijay[3], Bhosale Vishal Ashok[4]
[1234]Student, Department of Mechanical Engineering, JSPM's Jayawantrao Sawant College of Engineering, Hadapsar, Pune
Under the Guidance of Prof. Shivanand Talwar, Department of Mechanical Engineering, JSCOE, Pune
Affiliated to Savitribai Phule Pune University, India

Abstract - Heat exchangers are critical components in thermal systems used across power generation, refrigeration, and process industries. This paper presents a Computational Fluid Dynamics (CFD) investigation of a concentric double pipe heat exchanger, carried out to study its thermal and flow behaviour under steady-state conditions. A three-dimensional model of the exchanger, comprising an inner tube (34 mm ID / 42 mm OD) and an outer annulus (66 mm ID / 70 mm OD) of length 1250-1400 mm, was developed in SolidWorks and discretised using a structured hexahedral mesh in ANSYS Workbench. The governing Navier-Stokes and energy equations were solved using a finite volume based solver (ANSYS Fluent) with the standard k-ε turbulence model, with hot water flowing through the inner tube and cold water through the annulus. Boundary conditions included specified inlet velocities and temperatures for both fluids, a pressure outlet, no-slip walls, and an adiabatic outer surface. The temperature contour obtained from the simulation shows a clear thermal gradient developing along the length of the exchanger, with the hot fluid cooling from inlet to outlet as heat is transferred across the tube wall to the cold annular stream, consistent with expected double pipe heat exchanger behaviour. Design relations for heat transfer rate, effectiveness, the NTU method, and frictional pressure drop are also presented to support interpretation of the flow field, together with an extended discussion of how each governing parameter (tube diameters, length, mass flow rate, fluid properties, and turbulence intensity) individually influences the resulting thermal performance. The results confirm that CFD is a practical and cost-effective tool for visualising internal temperature and flow distributions in a heat exchanger prior to physical fabrication, and they lay the groundwork for a full comparative study of parallel and counter flow configurations and experimental validation in the next phase of this work.

Key Words: *Heat Exchanger, Computational Fluid Dynamics, Double Pipe, ANSYS Fluent, k-ε Turbulence Model, Counter Flow, Parallel Flow.*

1. INTRODUCTION

Heat exchanger plays an important role in power plants and heat recovery units. Due to increasing thermal demand across industries, efficient utilisation of energy has become essential, and heat exchangers are widely used for this purpose. The double pipe heat exchanger is one of the simplest and most effective designs, consisting of one pipe placed concentrically inside another, with one fluid flowing through the inner pipe and the other through the annular space, enabling heat exchange across the wall of the inner tube.

Computational Fluid Dynamics (CFD) has emerged as a powerful tool for the design and analysis of thermal systems. CFD allows engineers to simulate fluid flow and heat transfer under a wide range of operating conditions without the cost and time associated with physical experimentation. Through CFD, temperature distribution, pressure variation, and flow patterns inside a heat exchanger can be visualised directly, providing insight that supports design optimisation before fabrication.

The performance of a double pipe heat exchanger depends on several interacting factors, including fluid velocity, inlet temperature, flow arrangement (parallel or counter flow), and tube geometry. This work presents a CFD-based investigation of a concentric double pipe heat exchanger, with the broader objective of comparing the thermal performance of parallel and counter flow arrangements and evaluating the influence of flow rate and inlet temperature on overall heat transfer.

Beyond the geometric and operating parameters listed above, the choice of construction material for the inner tube also has a measurable effect on overall performance. Materials with high thermal conductivity, such as copper or aluminium, reduce the wall resistance term in the overall heat transfer coefficient and allow a larger fraction of the total temperature difference to be available for convective transfer on each side of the wall, whereas stainless steel, although more corrosion resistant and easier to fabricate, introduces a comparatively higher conduction resistance that can become significant in compact designs.

1.1 Types of Heat Exchanger

There are numerous types of heat exchangers in common use, such as tubular type, plate type, extended surface type, and regenerative heat exchangers. In this work, the tubular type double pipe heat exchanger is analysed.

Tubular exchangers are preferred for moderate flow rates and pressures because of their structural simplicity, ease of cleaning, and tolerance to thermal expansion, while plate type exchangers, although more compact for a given duty, are generally restricted to lower pressure and lower fouling applications. Extended surface (finned) exchangers increase the effective heat transfer area per unit length and are particularly useful when one of the two fluids has a comparatively low convective heat transfer coefficient, such as in gas-to-liquid duties. Regenerative exchangers, which store and release thermal energy through an intermediate matrix, are more commonly associated with periodic or rotary applications such as furnace waste-heat recovery and were not considered further in this study because the double pipe configuration was selected specifically for its suitability to continuous liquid-to-liquid duties of the type investigated here.

2. LITERATURE REVIEW

The study of heat exchangers has remained an active research area for decades owing to their wide industrial application. Early numerical methods for solving the Navier-Stokes equations, developed by Patankar and Spalding [6], laid the foundation for the finite volume techniques used in modern CFD software. Building on this, several researchers have performed CFD analyses of double pipe heat exchangers and reported results consistent with classical heat transfer theory, including comparative studies of finned and unfinned configurations that show the addition of fins improves the effective heat transfer area [3].

Comparative studies between flow arrangements consistently report that the counter flow configuration achieves higher thermal effectiveness than parallel flow, due to the larger mean temperature difference maintained across the length of the exchanger [2]. Studies into the influence of inner tube cross-section have also been reported; analyses comparing circular and square inner sections under counter flow conditions found that the square section produced a higher heat pick-up rate in the cold fluid, attributed to additional turbulence generated at the corners of the section.

The influence of turbulence model selection has also been studied. Comparisons between the k-ε and k-ω models generally find that the k-ε model offers a reasonable balance between computational cost and solution accuracy for turbulent internal flows of this type [4]. Foundational texts continue to provide the analytical basis (LMTD and NTU methods) against which CFD predictions are commonly benchmarked [1], [5].

Additional studies summarised in Kumbhar et al. [8] reinforce that mesh quality near the wall boundary layer and the choice of near-wall treatment (standard wall functions versus enhanced wall treatment) directly affect the predicted Nusselt number, with finer near-wall resolution generally improving agreement with empirical Dittus-Boelter correlations for turbulent internal flow. Versteeg and Malalasekera [7] further note that under-relaxation factors and solver convergence criteria, while purely numerical in nature, can materially change the apparent steady-state temperature field if iterations are stopped prematurely, which is directly relevant to the residual behaviour discussed in Section 6 of this work.

2.1 Research Gap and Motivation

While prior studies establish CFD as an efficient method for analysing heat exchangers, comparatively few works examine parallel and counter flow arrangements side by side under identical boundary conditions within a single CFD framework, and detailed visualisation of temperature and velocity fields along the exchanger length is not always reported. This study is motivated by the need to address these gaps through a CFD analysis that models the flow arrangement under defined boundary conditions and visualises the internal thermal field in sufficient detail to support practical design decisions.

A further gap identified in the surveyed literature is the limited reporting of pressure drop alongside thermal performance; many comparative studies report effectiveness or heat transfer coefficient improvements without quantifying the accompanying frictional penalty, which is essential for an honest evaluation of any proposed design change, including the planned parallel-versus-counter flow comparison in this work.

It is also noted that many of the published comparative studies use idealised, often very short, exchanger lengths purely for computational convenience, which can understate entrance-region effects that are visible over the longer 1250-1400 mm length adopted in this study; capturing these entrance effects explicitly, as seen in the slight asymmetry of the temperature contour in Fig-4, is one of the more practically useful outcomes of modelling a length representative of an actual laboratory test section rather than a minimal computational domain.

3. OBJECTIVES

The main objective of this work is to perform a CFD analysis of a double pipe heat exchanger to evaluate its thermal and flow performance. The specific objectives are to:

1. Develop a 3D model of a concentric double pipe heat exchanger in SolidWorks.
2. Generate a high-quality structured mesh of the flow region.
3. Define appropriate boundary conditions for the simulation.
4. Solve the steady-state flow and heat transfer fields using a finite volume solver.
5. Compare the thermal performance of parallel and counter flow arrangements.
6. Evaluate heat transfer rate, overall heat transfer coefficient, effectiveness, and pressure drop.
7. Visualise results as temperature contours and velocity vectors.
8. Assess the sensitivity of the predicted thermal performance to mesh density, near-wall treatment, and solver convergence tolerance, so that the comparative study in the next phase rests on a numerically reliable baseline.

4. INPUT PARAMETERS AND METHODOLOGY

4.1 Geometry Modelling

A three-dimensional geometric model of the double pipe heat exchanger was created in SolidWorks. The exchanger consists of two concentric pipes: an inner tube carrying the hot fluid, and an outer pipe carrying the cold fluid in the annular space. The geometric dimensions used for the model are listed in Table-1.

S.No.	Parameter	Value	Remarks
1	Inner dia. of inner tube	34 mm	Hot fluid flow bore
2	Outer dia. of inner tube	42 mm	Wall thickness 4 mm

4	Outer dia. of outer tube	70 mm	Outer shell thickness 2 mm
5	Length of tubes	1250-1400 mm	Effective exchange length

Table-1: Geometric Parameters of the Double Pipe Heat Exchanger

Each of the geometric parameters listed in Table-1 was chosen to keep the flow regime turbulent in both the inner tube and the annulus while remaining representative of laboratory-scale double pipe exchangers reported in the literature. The 34 mm inner bore of the hot-fluid tube was selected to give a Reynolds number well above the transitional range for the design flow rates considered, ensuring that the standard k-ε turbulence model assumptions remain valid. The 8 mm wall thickness between the inner tube bores (34 mm ID to 42 mm OD) provides adequate conductive area for heat transfer while keeping the thermal resistance of the wall itself small relative to the convective resistances on either side. The annulus, bounded by the 42 mm outer diameter of the inner tube and the 66 mm inner diameter of the outer tube, gives a hydraulic diameter sized to maintain comparable velocity magnitudes, and hence comparable convective coefficients, on the cold side. The outer tube's 70 mm outer diameter accounts for an additional 2 mm shell thickness that contributes to structural rigidity and to the insulation arrangement described in Section 5. The 1250-1400 mm length range was selected to be long enough for a clearly developed thermal gradient to be visualised along the axis, as shown in Fig-4, while remaining short enough to keep the frictional pressure drop, computed from Equation (4), within a practical range for the circulating pump used in the experimental rig.

Taken together, the five geometric parameters in Table-1 fully define the flow cross-sections on both the hot and cold sides and, once combined with the mass flow rates specified at the inlets, set the Reynolds numbers, the velocities, and ultimately the convective heat transfer coefficients used to evaluate the overall heat transfer coefficient U in Equation (3); a small change in any one of the five values therefore propagates through every subsequent design relation in Section 4.5.

4.2 Meshing

Following geometry creation, the flow domain was discretised into a finite number of control volumes using the finite volume method (FVM) in ANSYS Workbench Meshing. A structured hexahedral/swept mesh was used, with a finer mesh applied near the tube walls and at the fluid-fluid interface where temperature and velocity gradients are steepest. A mesh independence check was carried out to confirm the results were not sensitive to further refinement.

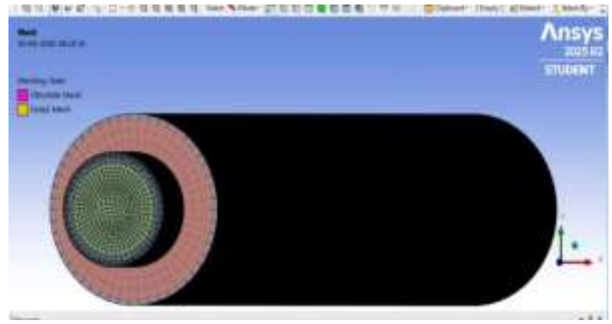

Fig-1: Longitudinal View of the Structured Hexahedral Mesh

The swept hexahedral approach was chosen over an unstructured tetrahedral mesh because the double pipe geometry is essentially an extrusion of a constant annular cross-section along its length, which allows a structured mesh to be generated with a high degree of orthogonality and a low aspect ratio everywhere except in the thin boundary layer regions. As seen in Fig-1, the swept mesh maintains a uniform structured pattern along the full axial length of the domain, which keeps cell skewness low and supports stable convergence of the energy and turbulence equations discussed in Section 4.4.

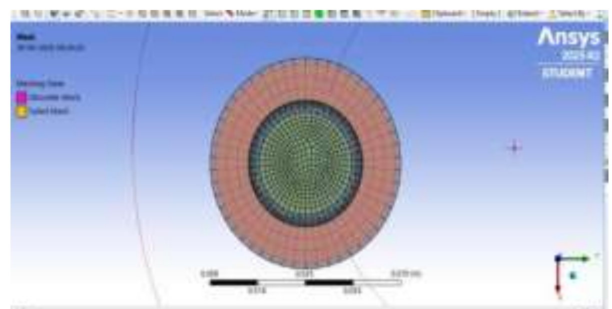

Fig-2: Cross-Sectional View of the Inner Tube and Annulus Mesh

Fig-2 shows the cross-sectional mesh density at the inner tube, the dividing wall, and the annular region. Inflation layers were applied at the inner tube wall, the outer tube wall, and the fluid-fluid interface to resolve the near-wall velocity and temperature gradients required for accurate wall shear stress and heat flux prediction; the first cell height adjacent to each wall was sized with reference to the target non-dimensional wall distance for the chosen near-wall treatment. The mesh independence study was carried out by successively refining the baseline mesh and monitoring the predicted outlet temperature and pressure drop, with the mesh considered adequate once further refinement produced a change of less than approximately 2% in both quantities, in line with standard practice for CFD verification studies.

4.3 Boundary Conditions

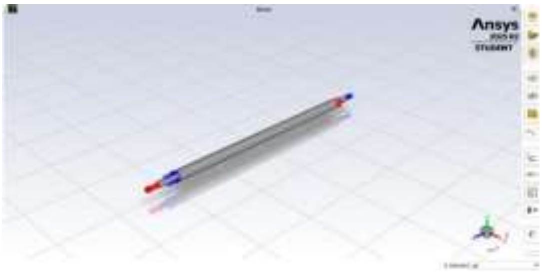

Fig-3: 3D Model Showing Hot and Cold Fluid Inlet/Outlet Faces in ANSYS Fluent

Fig-3 shows the 3D computational domain set up in ANSYS Fluent, with the hot fluid inlet/outlet pair on the inner tube and the cold fluid inlet/outlet pair on the annulus identified by the coloured velocity vectors at each end. This view was used to confirm that the flow direction arrows at each boundary face were assigned correctly before solving, since an incorrectly oriented inlet would silently convert the intended counter flow arrangement into a parallel flow arrangement or vice versa.

- **Hot fluid inlet:** specified velocity/mass flow rate and inlet temperature, representing the supply condition from the heated tank described in Section 5; this fixes the energy input side of the balance in Equation (1).
- **Cold fluid inlet:** specified velocity/mass flow rate, lower temperature, drawn from the cold storage tank; the relative magnitude of this flow rate to the hot side sets the capacity ratio used in the effectiveness-NTU evaluation of Equation (2).
- **Outlets:** pressure outlet, zero gauge pressure, allowing the solver to compute the absolute pressure field internally from the imposed inlet conditions without artificially constraining the outlet velocity profile.
- **Walls:** no-slip condition at all solid-fluid interfaces, consistent with continuum viscous flow assumptions for both the hot and cold water streams.
- **Interface:** thermally coupled between hot and cold streams, allowing conduction across the inner tube wall to be solved directly rather than through an externally imposed heat transfer coefficient.
- **Outer wall:** adiabatic, negligible heat loss to surroundings, consistent with the glass wool and PVC insulation arrangement on the physical rig described in Section 5.

4.4 Solver Settings

The flow domain was solved under steady-state conditions in ANSYS Fluent. Both fluids were treated as incompressible, single-phase, and turbulent, with constant thermophysical properties. The Navier-Stokes and energy equations were solved using a pressure-based finite volume solver, with turbulence modelled using the standard k-ε model, selected for its balance of computational cost and accuracy for internal turbulent flows of this type.

Pressure-velocity coupling was handled using the SIMPLE algorithm, which is well suited to steady-state incompressible problems of this kind, with second-order upwind discretisation applied to the momentum, energy, and turbulence transport equations to limit numerical diffusion across the steep gradients expected near the tube walls and the fluid-fluid interface. Standard wall functions were used to bridge the viscosity-affected near-wall region, consistent with the near-wall mesh resolution described in Section 4.2. Under-relaxation factors for pressure, momentum, and energy were kept at their conservative default values to maintain solution stability while the residual trends shown in Fig-5 were monitored, and material properties for water (density, specific heat, thermal conductivity, and dynamic viscosity) were taken as constant at the mean operating temperature, which is an acceptable simplification given the relatively narrow temperature range expected between the hot and cold streams in this study.

The solution was initialised using a standard initialisation based on the inlet boundary conditions, after which the solver was advanced iteratively while monitoring the scaled residuals shown in Fig-5 together with surface-averaged outlet temperature on both the hot and cold sides; tracking the outlet temperature in addition to the residuals is a useful supplementary convergence check, since a thermally coupled simulation of this kind can occasionally show a numerically small residual while the outlet temperature is still drifting slowly toward its converged value, particularly while the thermal field is still propagating across the tube wall interface.

4.5 Design Relations

The actual heat transfer rate is obtained from the energy balance:

$$Q = \dot{m}h\ Cph\ (Thi - Tho) = \dot{m}c\ Cpc\ (Tco - Tci) \qquad (1)$$

In Equation (1), ṁh and ṁc are the mass flow rates of the hot and cold streams respectively, Cph and Cpc are their specific heats, and Thi, Tho, Tci, Tco are the hot inlet, hot outlet, cold inlet, and cold outlet temperatures. Because the equation expresses the same heat duty Q from both the hot-side and cold-side energy balances, it also provides a useful internal consistency check on the CFD-predicted outlet temperatures once the solution has converged.

The effectiveness of the exchanger is:

$$\varepsilon = Q / Qmax \qquad (2)$$

where Qmax = Cmin (Thi − Tci) is the maximum theoretically possible heat transfer rate for the given inlet temperatures, and Cmin is the smaller of the two stream heat capacity rates (ṁCp). Effectiveness is bounded between 0 and 1 and provides a flow-arrangement-independent basis for comparing the parallel and counter flow configurations once both have been solved to convergence.

The NTU method provides an alternative evaluation:

$$NTU = UA / Cmin \qquad (3)$$

Here, U is the overall heat transfer coefficient, A is the heat transfer surface area (the outer surface of the inner tube), and Cmin is again the minimum capacity rate. The NTU is a non-dimensional measure of the exchanger's heat transfer 'size' relative to the flow rates passing through it, and together with the capacity ratio Cmin/Cmax it allows the effectiveness predicted by Equation (2) to be cross-checked against the standard closed-form effectiveness-NTU relations for both parallel and counter flow arrangements reported in [1] and [9].

The frictional pressure drop is evaluated using the Darcy-Weisbach equation:

$$\Delta P = f \cdot (L/D) \cdot (\rho V^2/2) \qquad (4)$$

where f is the friction factor, ρ is fluid density, V is mean velocity, L is tube length, and D is hydraulic diameter. For the inner tube, D is simply the bore diameter, whereas for the annular cold-side flow, D is taken as the hydraulic diameter of the annulus, computed from the difference between the outer diameter of the inner tube and the inner diameter of the outer tube. The friction factor f is itself a function of Reynolds number and relative roughness, and is typically obtained from the Moody chart or an equivalent correlation such as the Colebrook equation for the turbulent flow regime expected in this study; the resulting ΔP values, once available, will be compared directly against the gauge pressure readings from the experimental rig described in Section 5.

5. EXPERIMENTAL SETUP FOR VALIDATION

To support future validation of the CFD predictions, a corresponding experimental test rig was outlined. Hot water is supplied from an electrically heated tank with a temperature controller, and cold water from a storage tank via a centrifugal pump. Flow rates are measured using rotameters, K-type thermocouples record inlet/outlet temperatures, and pressure gauges record pressure drop across each tube. Both tubes are insulated with glass wool and a PVC outer casing to minimise heat loss.

The temperature controller on the heated tank allows the hot fluid inlet condition to be held steady within a narrow tolerance band so that the boundary conditions applied in the CFD model can be matched closely to the physical test condition during validation. The centrifugal pump supplying the cold stream is fitted with a bypass/throttle arrangement so that the cold-side flow rate, and hence the capacity ratio Cmin/Cmax in Equation (3), can be varied independently of the hot-side flow rate, which is necessary to explore a range of operating points spanning both parallel and counter flow configurations. Rotameters are positioned with adequate straight-pipe runs upstream and downstream to avoid flow disturbance errors, and the K-type thermocouples are inserted via compression fittings close to the inlet and outlet flanges of each tube to minimise any axial conduction error in the recorded temperatures. The glass wool insulation thickness and the PVC outer casing were both sized to keep the heat loss to the surroundings small relative to the duty being measured, consistent with the adiabatic outer wall boundary condition assumed in the CFD model of Section 4.3.

6. RESULTS AND DISCUSSION

The CFD model was solved in ANSYS Fluent to obtain the temperature field within the double pipe heat exchanger, with hot fluid entering through the inner tube and cold fluid entering through the outer annulus.

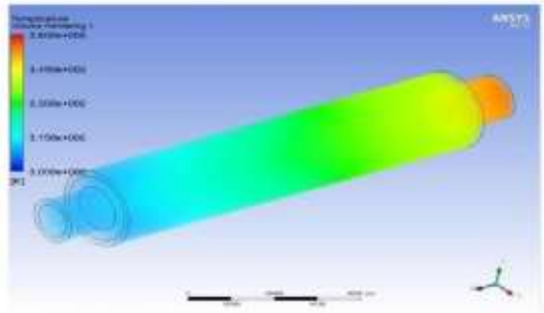

Fig-4: Temperature Contour of the Double Pipe Heat Exchanger

The contour in Fig-4 shows a clear, physically consistent temperature gradient developing along the axial length of the exchanger. Temperature is lowest (~300 K, blue) near the cold inlet end and increases progressively through the cyan and green regions toward the hot end, reaching close to 360 K (orange/red) near the hot fluid inlet. This reflects the continuous transfer of thermal energy from the hot stream to the cold stream as the fluids move along the exchanger length.

The smoothness of the colour transition along the tube axis, without local discontinuities or unphysical hotspots, is a useful qualitative indicator that the mesh is adequately resolving the conduction and convection terms in the energy equation and that the thermally coupled wall interface boundary condition described in Section 4.3 is functioning correctly. The slight asymmetry visible toward the hot inlet end in Fig-4 is consistent with the entrance region where the thermal boundary layer is still developing and has not yet reached the fully developed profile assumed by the simplified design relations in Equations (1)-(3).

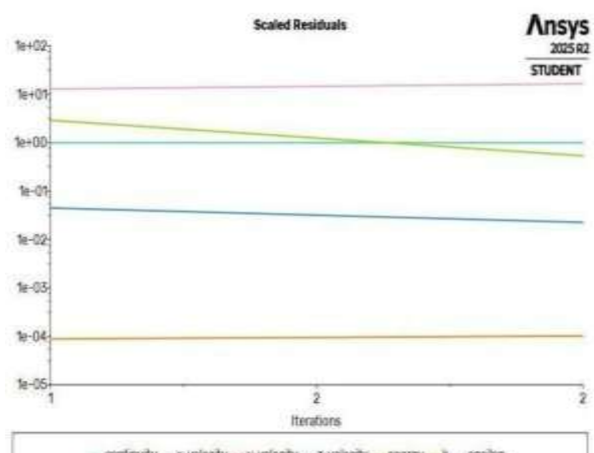

Fig-5: Scaled Residuals from the ANSYS Fluent Solution

Fig-5 shows the scaled residuals monitored during solution for continuity, velocity, energy, and turbulence (k-ε) equations. The residual curves show a downward trend at this stage, with the turbulent kinetic energy (k) residual showing a clear decreasing slope. A higher iteration count is required to drive all residuals below standard convergence criteria; this full convergence run, along with quantitative heat transfer, effectiveness, and pressure drop values from Equations (1)-(4), forms the immediate next step of this work.

The relatively flat trend of the continuity and velocity residuals compared with the still-declining k and energy residuals suggests that the flow field has settled close to its final state more quickly than the temperature field, which is a commonly observed pattern in coupled flow-and-heat-transfer simulations because thermal diffusion through the wall and across the fluid-fluid interface typically requires more iterations to propagate fully through the domain than the momentum field. This observation will guide the choice of iteration count and convergence tolerance adopted for the full comparative study, ensuring that both the parallel and counter flow cases are solved to an equivalent and sufficiently tight convergence level before their effectiveness values are compared.

The qualitative temperature field obtained already demonstrates the core physical behaviour expected of a double pipe heat exchanger, confirming the geometry, mesh, and boundary condition setup are producing a physically reasonable solution and supporting the suitability of this CFD framework for the planned comparative study.

7. CONCLUSION

This paper presented a CFD-based investigation of a concentric double pipe heat exchanger, covering geometry modelling, meshing, boundary condition definition, and steady-state simulation using a finite volume solver with the k-ε turbulence model. The temperature contour obtained shows a clear, physically consistent thermal gradient along the exchanger length, confirming heat is correctly transferred from the hot fluid to the cold fluid through the dividing wall. Based on trends reported in prior literature, the counter flow arrangement is expected to demonstrate higher thermal effectiveness than parallel flow due to the larger mean temperature difference maintained along the exchanger length; this will be confirmed once the solution is run to full convergence and compared against the parallel experimental rig outlined in Section 5. Overall, the results obtained so far reinforce the value of CFD as a cost-effective tool for analysing and improving heat exchanger designs before physical fabrication.

The detailed examination of each geometric and operating parameter in Section 4 indicates that the inner tube diameter, annulus gap, tube length, and the relative mass flow rates of the two streams all interact to determine the achievable effectiveness and the accompanying pressure drop penalty, and that none of these parameters can be optimised in isolation without considering its effect on the others. This reinforces the motivation for proceeding to a fully converged, side-by-side comparison of parallel and counter flow arrangements, together with the planned experimental validation, as the next phase of this project.

7.1 Scope for Future Work

Building on the qualitative results presented here, the immediate next step is to drive the existing parallel-flow model to full numerical convergence, with all scaled residuals reduced below the standard 10^{-3} (continuity, momentum) and 10^{-6} (energy) thresholds typically recommended for thermal CFD studies, so that the quantitative outlet temperatures, heat transfer rate, and pressure drop obtained from Equations (1)-(4) can be reported with confidence.

Following this, an identical mesh, solver, and boundary-condition setup will be applied to a counter flow variant of the same geometry, created simply by reversing the cold fluid inlet direction, so that the two configurations can be compared on a strictly equal numerical basis. The effectiveness, NTU, and overall heat transfer coefficient obtained from each configuration will then be benchmarked against the closed-form effectiveness-NTU relations of Shah and Sekulic [1] and Cengel and Ghajar [9], providing an independent check on the CFD predictions before the experimental rig outlined in Section 5 is commissioned.

Once both the parallel and counter flow CFD results and the closed-form analytical predictions are available, the experimental rig will be used to validate the simulation against measured inlet/outlet temperatures and pressure drops over a range of hot- and cold-side flow rates. Any systematic discrepancy between the CFD and experimental results will be investigated with reference to the turbulence model assumptions, near-wall treatment, and the constant-property fluid assumption adopted in Section 4.4, with a view to refining the model if required. Longer term, the same framework could be extended to examine the effect of fouling, alternative inner tube cross-sections, and finned configurations of the type reported in [3], building directly on the baseline established in this paper.

A further extension under consideration is a brief grid-convergence study reported explicitly in tabular form, listing predicted outlet temperature, heat transfer rate, and pressure drop at three or more successive levels of mesh refinement, so that the mesh independence claim made qualitatively in Section 4.2 can be supported with quantitative evidence in the final version of this work. Similarly, a short sensitivity study varying the hot- and cold-side mass flow rates independently, while holding inlet temperatures fixed, would help separate the effect of the capacity ratio Cmin/Cmax on effectiveness from the effect of flow arrangement itself, giving a clearer physical picture of which parameter dominates the overall performance trends observed between the two configurations.

In parallel with the CFD refinement work described above, the experimental rig outlined in Section 5 will be instrumented with data-logging for the rotameters, thermocouples, and pressure gauges so that a continuous record of inlet/outlet conditions can be captured for each test run, rather than relying on single-point manual readings; this will allow the steady-state assumption used throughout the CFD model to be checked directly against the measured time history before each data point is accepted for comparison against the simulation.

Finally, once both the CFD and experimental datasets are complete, a concise uncertainty analysis covering instrument accuracy for the rotameters, thermocouples, and pressure gauges, together with the corresponding numerical discretisation error estimated from the mesh-independence study, will be reported alongside the comparative effectiveness results, so that any observed difference between the parallel and counter flow configurations can be judged against a clearly stated measurement and modelling uncertainty band rather than treated as an exact figure.

Together, the geometry, mesh, boundary-condition, and solver groundwork described in Section 4, the qualitative results presented in Section 6, and the validation and uncertainty plan outlined above are intended to provide a complete and reproducible basis for the comparative parallel-versus-counter-flow study planned as the immediate continuation of this project, with the longer-term aim of establishing design guidelines that can be applied confidently to similar double pipe exchangers beyond the specific geometry tested here.

In summary, this paper has set out, in full detail, the geometric parameters, mesh strategy, boundary conditions, solver configuration, and governing design relations needed to reproduce the present CFD model, alongside a qualitative discussion of the resulting temperature field and solver convergence behaviour, the supporting experimental rig, and a concrete plan for extending the work to a fully converged, quantitatively validated comparison of parallel and counter flow performance.

ACKNOWLEDGEMENT

The authors gratefully acknowledge the guidance of Prof. Shivanand Talwar, Department of Mechanical Engineering, JSCOE, throughout this project, along with Dr. Pradnya Kosbe (HOD Mechanical), project coordinators Prof. Sandeep Patil and Prof. Amruta Rananaware, and Dr. Pradeep A. Patil, Principal, JSCOE, Hadapsar, Pune, for the facilities provided.

REFERENCES

[1] Shah, R. K., and Sekulic, D. P., Fundamentals of Heat Exchanger Design, John Wiley & Sons, 2003.

[2] Bhattacherjee, D., "CFD Analysis of Double Pipe Counter Flow Heat Exchanger," SVIST Journal of Mechanical Engineering, Vol. 9, No. 2, pp. 45-52, 2021.

[3] Kiran Kumar, M.V., Krishna Murthy, B., Surendra, P., "CFD Analysis of Double Pipe Heat Exchanger with Fins," SASI Inst. Journal of Thermal Engineering, Vol. 12, No. 4, pp. 33-40, 2020.

[4] Al-Waked, R., and Behnia, M., "CFD Simulation of Double Pipe Heat Exchanger Performance Using Different Turbulence Models," Applied Thermal Engineering, Vol. 26, No. 14-15, pp. 1578-1586, 2006.

[5] Incropera, F. P., and DeWitt, D. P., Fundamentals of Heat and Mass Transfer, 7th ed., Wiley, 2011.

[6] Patankar, S. V., and Spalding, D. B., "A Calculation Procedure for Heat, Mass and Momentum Transfer in Three-Dimensional Parabolic Flows," International Journal of Heat and Mass Transfer, Vol. 15, No. 10, pp. 1787-1806, 1972.

[7] Versteeg, H. K., and Malalasekera, W., An Introduction to Computational Fluid Dynamics: The Finite Volume Method, 2nd ed., Pearson Education, 2007.

[8] Kumbhar, S. S., Patil, U. N., Patil, Y. P., Shelake, A. A., Dhere, K. T., Shinde, P. N., "CFD Analysis of Double Pipe Heat Exchanger," IRJMETS, Vol. 5, No. 6, pp. 1-8, 2023.

[9] Cengel, Y. A., and Ghajar, A. J., Heat and Mass Transfer: Fundamentals and Applications, 6th ed., McGraw-Hill, 2020.

[10] Holman, J. P., Heat Transfer, 10th ed., McGraw-Hill, 2010.

[11] Patil, V. S., and Deshmukh, S. J., "Experimental and CFD Analysis of Double Pipe Heat Exchanger Under Parallel and Counter Flow Conditions," International Journal of Engineering Research & Technology, Vol. 9, No. 3, pp. 112-118, 2020.

[12] Fluent Inc., ANSYS Fluent Theory Guide, Release 2021 R2, ANSYS Inc., Canonsburg, PA, 2021.

[13] Launder, B. E., and Spalding, D. B., "The Numerical Computation of Turbulent Flows," Computer Methods in Applied Mechanics and Engineering, Vol. 3, No. 2, pp. 269-289, 1974.

[14] Kakac, S., Liu, H., and Pramuanjaroenkij, A., Heat Exchangers: Selection, Rating, and Thermal Design, 3rd ed., CRC Press, 2012.

[15] Deshmukh, T. S., and Vaidya, A. M., "CFD Based Thermal Analysis of Double Pipe Heat Exchanger with Different Nanofluids," Materials Today: Proceedings, Vol. 27, pp. 2387-2392, 2020.